วิศวกรรมสาร มข.ปีที่ 36 ฉบับที่ 1 (77-85) มกราคม – มีนาคม 2552 บทความวิจัย
KKU Engineering Journal Vol.36 No.1 (77-85) January – March 2009

Input Shaping to Reduce Vibration in Human-Operated Very-Flexible-Link Robot Manipulator

Withit Chatlatanagulchai[* 1)] and Chonlawit Prutthapong[2)]

ABSTRACT

Human-operated manipulators, such as construction crane, gantry crane, and tele-operated robot manipulator, are refrained from fast slewing because of the vibrations of its link and payload. To be long, light, fast, and to carry large payload, the manipulator's natural frequencies fall within the controller bandwidth resulting in resonance. In this paper, we apply the input shaping technique, in which the reference position signal is convolved with a properly designed impulse sequence to avoid exciting the natural frequencies, to a very-flexible-link robot manipulator to significantly reduce vibration. The technique is in real-time; therefore, the given reference position can be arbitrary and need not be known a priori, which suits the human-operated setting. Experimenting with a scale-down robot confirms the effectiveness of the technique in reducing slewing vibration. The result can be readily extended to a much-larger human-operated manipulator that vibrates.

Keywords: Vibration Reduction, Flexible Link, Input Shaping, Shaped Reference Input, Convoluti

* 1) Lecturer, Control of Robot and Vibration Laboratory (CRV Lab),
Department of Mechanical Engineering, Faculty of Engineering, Kasetsart University,
E-mail: fengwtc@ku.ac.th

2) Commander, Auxiliary Engine Factory, Naval Dockyard, Navy

Introduction

Economically we would like to have a long, light, fast, and high-capacity manipulator. The lightness reduces the control effort used. Being long enables the manipulator to cover more area. Able to move fast and carry more payload improve productivity.

However, the lighter structure brings about more link flexibility, an equivalence to inserting softer spring into the link. Meanwhile, being lengthy and carrying more payload increase link inertia and tip mass. The softer spring and the increasing inertia lower the natural frequencies. If too much, they can be within the controller bandwidth and be excited by the control input causing severe oscillation. On the other hand, the robot cannot move fast when the link is flexible because that requires the increase of the controller bandwidth.

To obtain the fast movement of the flexible-link robot, one must either modify physical structure to have higher natural frequencies and damping ratio, design controller to actively counteract the oscillation, or avoid exciting the low natural frequencies.

Wang and Russell (1995) studied optimum shape of the robot's link to increase the fundamental frequency under a finite range of tip loads. Pratiher and Dwivedy (2008) studied the nonlinear behavior of a single-link flexible visco-elastic manipulator. The visco-elastic material has good vibration absorbing behavior. Nevertheless, modifying the physical structure is neither convenient since it involves redesigning the whole structure, which may not be economical for some large manipulators, nor effective under payload variation.

Active controllers exert external energy on the robot to control its response. Present works include either linear or nonlinear systems consisting of fixed or adaptive models and adaptive or robust controllers. The most common controllers are those of computed-torque method ((Singh, 1998), (Chapnik *et al.*, 1993), (Jnifene and Fahim, 1997)), gain scheduling method ((Carusone *et al.*, 1993), (Konno and Uchiyama, 1995)), and intelligent-system method ((Moudgal *et al.*, 1994), (Caswara *et al.*, 2002).) Using active controllers, though effective in reducing the vibration, requires external energy or additional actuators, hence increasing operating cost.

To avoid exciting the natural frequencies, either reference or control inputs can be altered so that no energy is injected around the flexible modes either by construction of input from versine or ramped sinusoidal functions ((Meckl and Seering, 1988), (Chatlatanagulchai *et al.*, 2006)) or by using a notch filter (Singer and Seering, 1988) or by convolution of the input with a sequence of impulses ((Smith, 1957), (Singer and Seering, 1990).) These so-called command or input shaping methods have been used by only a limited group of researchers.

In this paper, we apply the convolution input shaping method to our human-operated very-flexible-link robot. This laboratory-scale robot is made to follow any arbitrary angular position commanded by human. First, several natural frequencies were obtained from pulse excitation using a hammer. Then, corresponding damping ratios were obtained by inputting frequency-varying sine wave to the robot and measuring its steady-state response amplitude. The damping ratio of a particular natural frequency can be found from two surrounding frequencies with half-power amplitudes. Once the natural frequencies and the damping ratios are determined, they can be used to design an impulse sequence whose convolution with the reference position input produces less energy around the natural frequencies. This

impulse sequence itself is a convolution of several impulse sequences each designed for a specific natural frequency. A real-time algorithm for convolution of an arbitrary signal with impulse sequence was devised, which enables the robot to follow arbitrary position commanded by human. A PI controller is used in the closed-loop system for tracking whereas the shaped reference input is used to reduce the excitation of the natural frequencies for less vibration.

Comparing the shaped and unshaped cases, the experimental results show that, with shaped reference input, the robot can follow the human command closely with significantly less vibration. Hence the robot can achieve faster point-to-point motion despite its very flexible link. The design can be extensively applied to actual cranes or industrial robot manipulators for faster move and reducing link damage due to vibration. Comparing to the active controller method, this method requires less amount of control input hence less operating cost.

The paper is organized as follows. In the next section, we provide some basics of the input shaping method. Then, we discuss determination of the robot's natural frequencies and damping ratios, followed by details of input shaping for this particular robot. Then, the experimental set-up and results are presented. Conclusions are given in the last section.

Input Shaping Basics

The impulse response of an underdamped system is given by

$$y(t)=\frac{\hat{F}_1 e^{-\zeta\omega_n(t-t_1)}}{m\omega_n\sqrt{1-\zeta^2}}\sin\sqrt{1-\zeta^2}\,\omega_n(t-t_1),$$

where $\hat{F}_1$ is impulse magnitude, y is the response, ζ is damping ratio, ω_n is natural frequency, m is mass, and t_1 is the time the impulse applies. A properly designed impulse magnitude $\hat{F}_2$ can be applied at a time t_2 to produce a response that cancels with that of $\hat{F}_1$ as shown in Figure 1.

Instead of two, it can be shown that the amplitude of the sum of N impulse responses is given by

$$A=\sqrt{\left(\sum_{i=1}^{N}A_i\cos\beta_i\right)^2+\left(\sum_{i=1}^{N}A_i\sin\beta_i\right)^2} \quad (1)$$

with $A_i=\hat{F}_i e^{-\zeta\omega_n(t-t_i)}/\left(m\omega_n\sqrt{1-\zeta^2}\right)$

and

$$\beta_i=\sqrt{1-\zeta^2}\,\omega_n t_i.$$

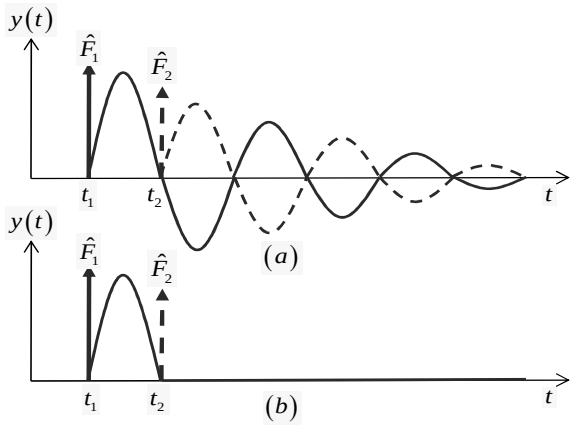

Figure 1 *System response of two impulses.*

To have zero vibration, setting (1) to zero and t to t_N results in two constraints

$$\sum_{i=1}^{N}\hat{F}_i e^{-\zeta\omega_n(t_N-t_i)}\cos\sqrt{1-\zeta^2}\,\omega_n t_i=0 \quad (2)$$

and

$$\sum_{i=1}^{N}\hat{F}_i e^{-\zeta\omega_n(t_N-t_i)}\sin\sqrt{1-\zeta^2}\,\omega_n t_i=0. \quad (3)$$

For two impulses, of which the first one applies at $t_1=0$ and its impulse magnitude normalizes to $\hat{F}_1=1$, $\hat{F}_2$ and t_2 can be found from the two equations above.

Since the amount of residual vibration left depends on the accuracy of the natural frequency ω_n and the damping ratio ζ used to compute $\hat{F}_2$ and t_2, to increase the robustness of the input under variations of the natural frequency, we can set the derivatives, with respect to ω_n, of (2) and (3) to zeros to obtain two more constraints

$$\sum_{i=1}^{N} \hat{F}_i t_i e^{-\zeta\omega_n(t_N - t_i)} \cos\left(\sqrt{1-\zeta^2}\,\omega_n t_i\right) = 0 \qquad (4)$$

and

$$\sum_{i=1}^{N} \hat{F}_i t_i e^{-\zeta\omega_n(t_N - t_i)} \sin\left(\sqrt{1-\zeta^2}\,\omega_n t_i\right) = 0. \qquad (5)$$

The constraints (4) and (5) reduce the sensitivity of the constraints (2) and (3) to change in ω_n and can be used to solve for two additional unknowns t_3 and $\hat{F}_3$ of the third impulse. It can be shown that these constraints also apply to the robustness of the input under variations of the damping ratio.

Letting $t_1 = 0$ and $\hat{F}_1 = 1$, we can compute $t_2, \hat{F}_2, t_3,$ and $\hat{F}_3$ from (2)-(5) to be

$$t_2 = \frac{\pi}{\omega_n\sqrt{1-\zeta^2}},\ \hat{F}_2 = 2e^{\frac{-\zeta\pi}{\sqrt{1-\zeta^2}}},\ t_3 = \frac{2\pi}{\omega_n\sqrt{1-\zeta^2}},$$

and $\hat{F}_3 = e^{\frac{-2\zeta\pi}{\sqrt{1-\zeta^2}}}$. (6)

The resulting three-impulse sequence can be convolved with the reference position r to create a shaped input that will cancel the residual vibration. Normally, if the controller in the closed-loop system does not add any underdamped poles, the natural frequency and damping ratio of the closed-loop system will remain the same as those of the plant.

For tracking, we need all impulse amplitudes to sum to one so that the shaped reference position will have the same end point as that of the original reference position.

Input Shaping of a Very-Flexible-Link Robot

A diagram of a one-link flexible-link robot is given in Figure 2. The $x_0 - y_0$ frame is the inertia frame whereas the $x - y$ frame is attached to a base, which is driven by a motor. Let θ be the base angle, α be the payload angular position to be controlled, $\ddot{s}$ be the tip linear acceleration, and v be the input voltage to the motor amplifier.

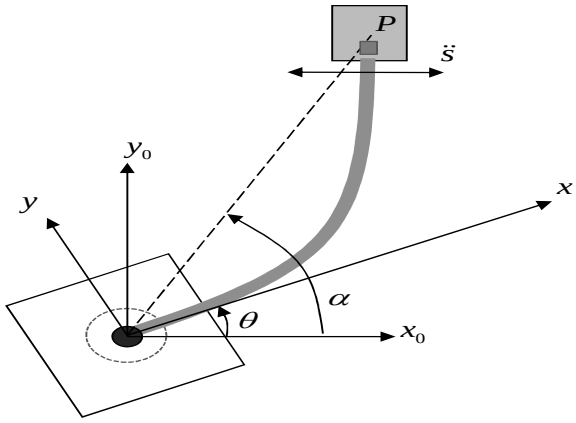

Figure 2 *Diagram of a one-link flexible-link robot.*

To find the natural frequencies, the link is hit by a hammer at one end. The deviation of the tip angular position, measured by three strain gauges, is recorded at the other end. The power spectrum of the deviation signal, which is proportional to $\alpha - \theta$, is given in Figure 3. The first five natural frequencies are identified as $\omega_1 = 8.5\ rad/s$, $\omega_2 = 19\ rad/s$, $\omega_3 = 38\ rad/s$, $\omega_4 = 56\ rad/s$, and $\omega_5 = 75\ rad/s$. By considering a closed-form solution of an exact model (Iemsamai and Chatlatanagulchai, 2008), we can see that the first three natural frequencies constitute about 97% of the solution; therefore, it is sufficient to shape the input on these three frequencies.

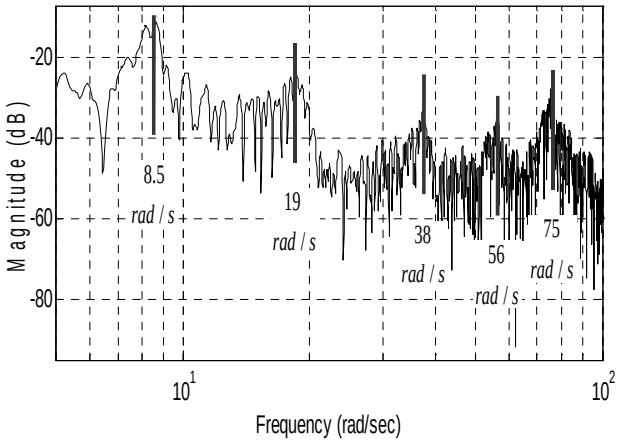

Figure 3 *Power spectrum of the tip angular position signal when the robot is excited by a hammer. The vertical lines mark the first-to-fifth-mode natural frequencies.*

To determine the damping ratio corresponding to each natural frequency, the harmonic response curve is plotted by varying the frequency of the sine-wave input to the motor and recording steady-state vibration amplitude of $\alpha - \theta$. The two frequencies ω_{i1} and ω_{i2}, which are the half-power points of each natural frequency ω_i, are noted, and the damping ratio ζ_i can be found from the formula

$$\frac{1}{2\zeta} = \frac{\omega_i}{\omega_{i2} - \omega_{i1}},$$

where $i = 1, 2,$ and $3.$ The damping ratios corresponding to the first three natural frequencies are found to be $\zeta_1 = 0.01,$ $\zeta_2 = 0.05,$ and $\zeta_3 = 0.0294.$

For each natural frequency, timing and amplitudes of the corresponding impulse sequence are given by (6). Since we use three impulses per frequency for three frequencies, the convolution among the three impulse sequences produces a sequence of 27 impulses. This off-line convolution can be performed by any suitable engineering software, for example, the Matlab command *conv*. These impulses are then normalized to sum to one. The result is given in Figure 4.

Once designed, this impulse sequence is fixed. Any arbitrary reference position signal will be convolved in real-time with the impulse sequence to create a shaped reference position for the plant to track. This shaped reference position will have the same effect in cancelling the residual vibration as that of the impulse sequence. Figure 5 shows the resulting shaped input (the solid line) after convolving a square-wave reference position (the dash line) with the impulse sequence in Figure 4.

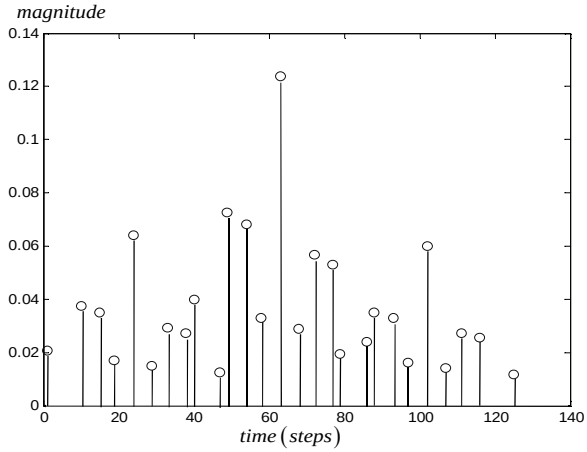

Figure 4 *Normalized impulse sequence to be convolved with reference position signal.*

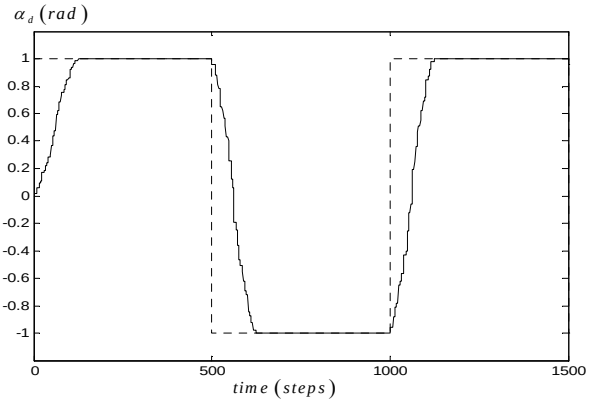

Figure 5 *Square-wave (unshaped) reference position is the dash line. Its convolution with the impulse sequence (shaped) is the solid line.*

Experimental Set-Up and Results

Figure 6 is a photograph of our flexible-link robot. An accelerometer, to measure the tip linear acceleration $\ddot{s}$, is mounted next to the payload whose location is at the tip. The payload is varying due to the jiggling movement of some coins inside. This payload variation contributes to uncertainties in the system's natural frequencies and damping ratios. It is to be seen that the third impulse in (6) effectively reduces the sensitivity to these uncertainties. Three strain gauges are used to measure the transversal deflection $\alpha - \theta$, and an optical encoder is used to measure the base angular position θ. A steel ruler is used as the flexible link with an effective length of 0.54 m.

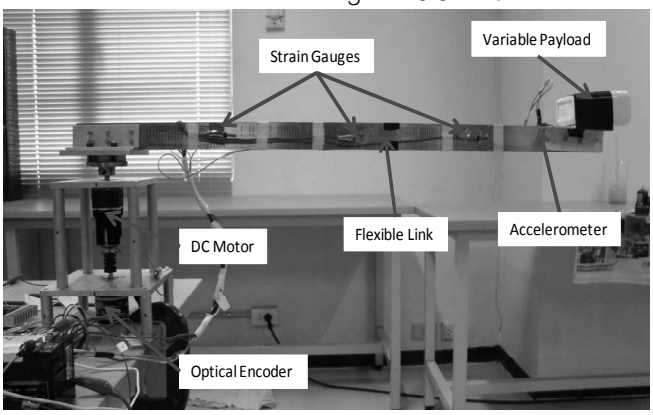

Figure 6 *Photograph of the flexible-link robot in our laboratory.*

Figure 7 is a block diagram of the experimental arrangement. A host computer, running Labview and Matlab software, is used to communicate with user and a target computer. The impulse sequence is designed off-line using Matlab. The real-time hardware-in-the-loop experiment is performed using Labview.

A target computer contains a data acquisition card whose functions are to acquire sensor signals and to send out actuator command from the control algorithm. Four analog input (AI) channels, one analog output (AO) channel, and one counter channel are used in the experiment. The target runs a Labview Real-Time operating system.

The host and target computers are connected to each other via a LAN line. Control signal is sent as voltage to a motor amplifier board to amplify to a level that can drive the DC motor. An IC chip accelerometer is mounted at the tip to measure linear acceleration. There is an in-house-design op-amp circuit to amplify strain gauges' signals. A DC power supply supplies required current to the motor amplifier board.

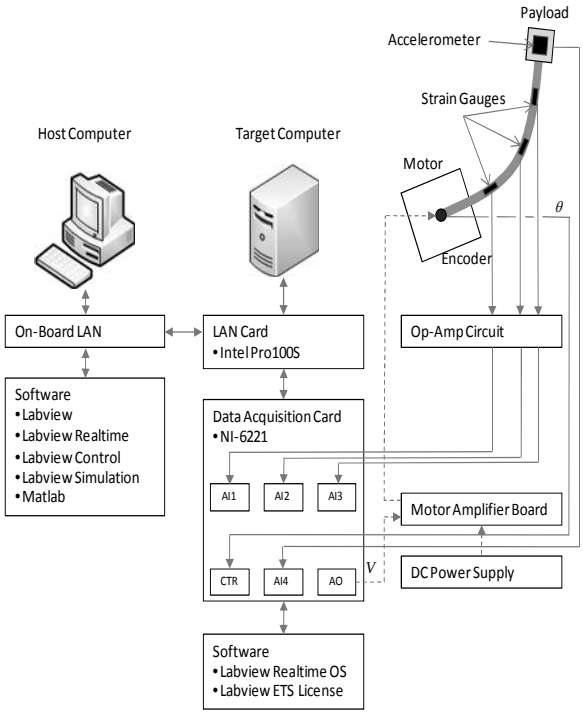

Figure 7 Block diagram of the experimental set-up and associated hardware.

The sampling time of $10\,ms$ is used for the hardware. The closed-loop controller is a simple PI controller with $K_p = 0.05$ and $K_I = 0.01.$ This controller does not change the natural frequency and the damping ratio of the closed-loop system from those of the plant. The impulse sequence in Figure 4 must convolve in real-time with any incoming reference position command given by human.

To do that, let $IS(t)$ represent an impulse sequence of n impulses, it can be expressed in the time domain as

$$IS(t) = \sum_{i=1}^{n} A_i \delta(t - t_i),\ 0 \le t_i < t_{i+1},$$

where $\delta(t)$ is the Dirac delta function, A_i and t_i are the amplitude and time of the i^{th} impulse.

Suppose we want to convolve this impulse sequence with a step reference input $r(t)$. The convolution is given by

$$IS * r = \int_{-\infty}^{\infty} IS(\tau) r(t-\tau)\, d\tau.$$

Since $r(t-\tau) = r(-\tau+t)$ can be viewed as a mirror image of $r(\tau)$ about the vertical axis shifting by the amount of t, the convolution result can be obtained graphically as Figure 8. Figure 8(a) shows $IS(\tau)$ and $r(\tau)$. Figure 8(b) plots the mirror image $r(-\tau)$. Note that the arrow of $r(\tau)$ marks the more current time step of the signal. Figure 8(c) is when $r(-\tau)$ is shifted by t. Finally, Figure 8(d) shows the resulting convolution $IS * r$.

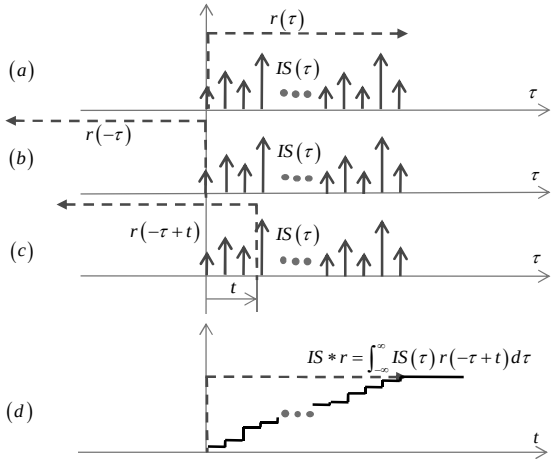

Figure 8 *Graphical interpretation of the convolution process.*

Our impulse sequence in Figure 4 has 27 impulses spanning 127 time steps, when one time step equals one sampling period of $0.01\,s$. In real-time convolution, 127 shift registers are added in the Labview program to store the current reference command $r(t_{current})$ as well as its previous 126 values. This reference command is given to the system in real-time by a human operator. A fixed array containing the impulse sequence is multiplied by the reference command stored in the shift registers. By doing this way, the most current command is multiplied by the first impulse, and the subsequent commands are multiplied by the subsequent impulses as shown in Figure 8(c).

A toggle switch is written in the program to turn the input shaper on and off. A turnable knob is also added to the program to let an operator control the robot as desired. The readings from the knob are interpreted as the reference position to be followed by the robot's payload position α. Figure 9 shows a human operator commanding the robot.

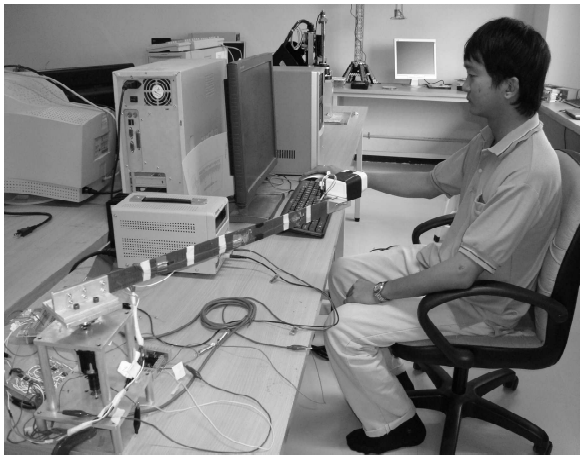

Figure 9 *A human operator commands the robot to move to arbitrary positions.*

Figure 10 plots the robot's payload position α versus its desired trajectory α_d given arbitrarily by the operator. By alternating between the shaped and unshaped reference inputs, we clearly see that, with shaped input, the robot was able to settle faster with significantly less vibrations than with the unshaped case, which suffers from severe residual vibration.

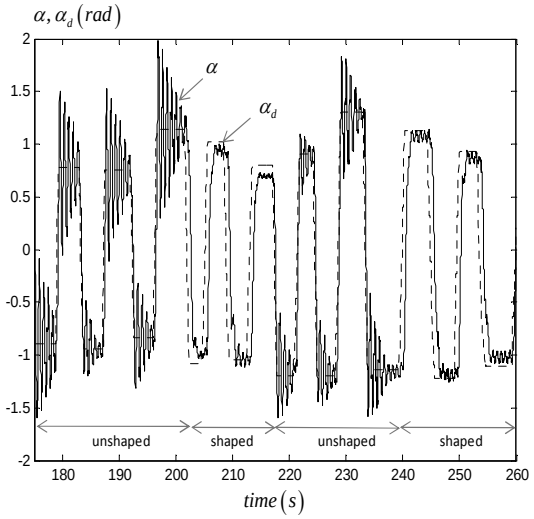

Figure 10 *Tracking result for the shaped and unshaped cases: angular position output* α *(solid line) and its desired value* α_d *(dash line.)*

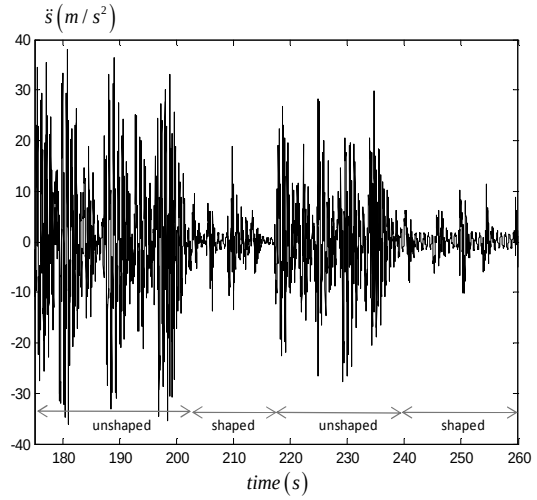

Figure 11 *Tip acceleration for shaped and Unshaped case*

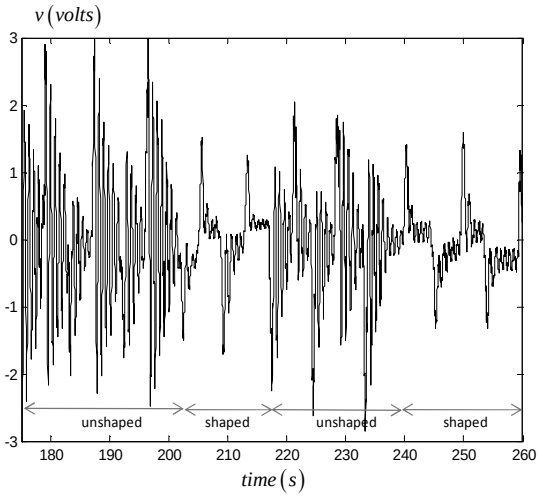

Figure 12 *Control input to the motor amplifier for shaped and unshaped cases.*

Figure 11 shows the signal from the accelerometer at the tip, with significantly higher acceleration output seen during the unshaped periods. The root-mean-square value of the acceleration is found to be 10 times higher during the unshaped period than during the shaped period.Figure 12 contains the control input voltage to the motor amplifier. The control input is more chattering with higher amplitude during the unshaped period. A video clip of the robot in operation can be downloaded from http://www.crvlab.eng.ku.ac.th/, under *research* menu.

Conclusions

Using the shaped reference position, a very-flexible-link robot can move with significantly less vibration. Since the settling time is reduced, the robot achieves faster move time while using lower amount of actuator activity.

The technique can be implemented with existing manipulators such as construction crane, gantry crane, or industrial mechanisms, without much effort. The only information required for the method is the system's natural frequencies and damping ratios, which can be conveniently obtained from non-destructive experiments.

Since the method relies on the superposition principle of the linear system, it is doubtful that the method will ever be implemented in nonlinear setting. However, more research efforts should be spent on on-line identification of the natural frequencies and damping ratios since these values are vital to the effectiveness of the method. Various robust controllers can also replace the simple PI controller in the closed-loop system to provide better robustness against system variations.

Acknowledgement

This work is performed at the Control of Robot and Vibration Laboratory, which is situated at and partially supported by the Research and Development Institute of Production Technology (RDiPT) of Kasetsart University, Thailand.

References

Carusone J., Buchan K. S., and D'Eleuterio G. M. T. 1993. Experiments in end-effector tracking control for structurally flexible space manipulators. **IEEE Trans. on Robotics and Automation**. 9, 5: 553-560

Caswara F. M. and Unbehauen H. 2002. A neurofuzzy approach to the control of a flexible-link manipulator. **IEEE Trans. on Robotics and Automation**. 18, 6(December): 932-942

Chapnik B. V., Heppler G. R., and Aplevich J. D.1993. Controlling the impact response of a one-link flexible robotic arm. **IEEE Trans. on Robotics and Automation**. 9, 3(June): 346-351

Chatlatanagulchai W., Beazel V. M., and Meckl P. H. 2006. Command shaping applied to a flexible robot with configuration-dependent resonance. **Proc. of the 2006 American Control Conference**. Minneapolis. MN.

Iemsamai K. and Chatlatanagulchai W. 2008. Exact mathematical model of a flexible-link robot. **of the 22nd Conference of Mechanical Engineering Network of Thailand**. Patumthani.

Jnifene A. and Fahim A. 1997. A computed torque/time delay approach to the end-point control of a one-link flexible manipulator. **Dynamics and Control**. 7:171-189

Konno A. and Uchiyama M. 1995. Vibration suppression control of spatial flexible manipulators. **Control Eng. Practice**. 3, 9: 1315-1321

Meckl P. H. and Seering W. P. 1988. Reducing residual vibration in systems with uncertain resonances. **Contr. Syst. Mag**. 8, 2: 73-76

Moudgal V. G., Passino K. M., and Yurkovich S. 1994. Rule-based control for a flexible-link robot. **IEEE Transactions on Cont. Sys. Tech**. 2, 4: 392-405

Pratiher B. and Dwivedy S. K. 2008. Non-linear vibration of a single link viscoelastic Cartesian manipulator. **International Journal of Non-Linear Mechanics**. 43: 683-696

Singer N. C. and Seering W. P. 1988. Using acausal shaping techniques to reduce robot vibrations. **Proc. IEEE Int. Conf. Robotics Automat**. 1434-1439

Singer N. C. and Seering W. P. 1990. Preshaping command inputs to reduce system vibration. **ASME Trans. J. Dynam., Meas., Contr**. 112, 1(March): 76-82

Singh S. N. 1988. Control and stabilization of a nonlinear uncertain elastic robotic arm. **IEEE Trans. on Aerospace and Electronic Systems**. 24, 2(March): 148-155

Smith O. J. M. 1957. Posicast control of damped oscillatory systems. **Proc. of the IRE**. 45(September): 1249-1255

Wang F. Y. and Russell J. L. 1995. Optimum shape construction of flexible manipulators with total weight constraint. **IEEE Trans. on Systems, Man, and Cybernetics**. 25, 4(April): 605-614